remote sensing

MDPI

Article

A Comparison of the Performance of Bias-Corrected RSMs and RFMs for the Geo-Positioning of High-Resolution Satellite Stereo Imagery

Zhonghua Hong [1,2], Xiaohua Tong [2,*], Shijie Liu [2], Peng Chen [2], Huan Xie [2] and Yanmin Jin [2]

Received: 9 October 2015; Accepted: 5 December 2015; Published: 10 December 2015
Academic Editors: Gonzalo Pajares Martinsanz, Richard Müller and Prasad S. Thenkabail

1 College of Information Technology, Shanghai Ocean University, 999 Hu-Chenghuan Road, Shanghai 201306, China; zhhong@shou.edu.cn
2 College of Surveying and Geo-Informatics, Tongji University, 1239 Siping Road, Shanghai 200092, China; liusjtj@gmail.com (S.L.); chenpeng@tongji.edu.cn (P.C.); huanxie@tongji.edu.cn (H.X.); jinyanmin@yeah.net (Y.J.)
* Correspondence: xhtong@tongji.edu.cn; Tel: +86-21-6598-8851; Fax: +86-21-6598-1085

Abstract: High-resolution stereo satellite imagery is widely used in environmental monitoring, topographic mapping, and urban three-dimensional (3D) reconstruction. However, a critical issue in these applications using high-resolution stereo satellite imagery is to improve the accuracy of point geo-positioning. This paper presents a framework for comparison of the performance of the three-dimensional (3D) geo-positioning of the bias-corrected Rigorous Sensor Models (RSMs) and rational function models (RFMs) with respect to the high-resolution QuickBird stereo images in three spaces (*i.e.*, orbital space, image space and object space). The compared models include a bias-corrected RSM in the orbital space, a bias-corrected RSM and RFM in the image space, and a bias-corrected RSM and RFM in the object space. In the comparison, the RSMs and RFMs use the vendor-provided orbit data and Rational Polynomial Coefficients (RPCs), respectively. The experimental results indicated that, (1) these five bias-corrected models can provide a sub-pixel geo-positioning accuracy. With the zero-order polynomial correction model in the orbital space and a minimum of three Ground Control Points (GCPs), the accuracy based on RPCs better than 0.8 m in horizontal direction and 1.3 m in vertical direction. With an increase in the number of GCPs, or in the order of correction models, the regenerated orbital parameters achieve a slight improved positioning accuracy of 0.5 m in horizontal direction and 0.8 m in vertical direction with 25 GCPs, which indicates that the low-order correction model in the orbital space can accurately model the effects of ephemeris and attitude errors; (2) the performances of bias-corrected RSM and RFM in image space are rather similar. However, the bias-corrected RSM and RFM in image space achieve a better accuracy than the bias-corrected RSM and RFM in object space, with the same configuration of GCPs.

Keywords: bias-correction; RSM; RFM; geo-positioning; high-resolution satellite imagery; accuracy

1. Introduction

The rapid development of High-Resolution Satellite Imagery (HRSI), such as QuickBird and IKONOS, has provided a large number of applications in environmental monitoring, topographic mapping, and urban three-dimensional (3D) reconstruction with a sub-meter spatial resolution. However, one of the most critical issues with respect to these applications is to improve the geo-positioning accuracy of stereo imageries. In general, there are two kinds of geometric sensor orientation models for HRSI. The first one is the Rigorous Sensor Model (RSM) [1,2], and the second

is the Rational Function Model (RFM) [3]. The purpose of these two sensor models is to reconstruct the transformation of the points between the 3D object space and image space.

The RSM, which is based on the collinearity condition, is considered as the most rigorous geo-positioning model, particularly when used in bundle adjustment. The RSM includes interior and exterior orientation parameters of the acquired image [4,5]. The former parameters can be interpreted directly from the vendor-provided image metadata, and the latter need to be interpolated by both ephemeris data and attitude data of the satellite, by the use of least squares adjustment [6] or Lagrange interpolation [7]. However, in practice, the RSM may not be an efficient model because of its sophisticated parameter definition, complicated mathematical expression, and self-correlation of exterior orientation elements [8,9]. In contrast, the RFM is a generalized sensor model that uses the ratio of polynomials and is regarded as an alternative to the RSM [10]. This model has the benefit of low computational complexity, a closed form solution, and equivalent accuracy to the RSM [11].

According to a number of reports on the geo-positioning accuracy of QuickBird imagery [4,8,12–14], both the RSM and RFM can achieve an accuracy of 16–25 m without Ground Control Points (GCPs). The reason for this result is that systematic errors can exist in the vendor-provided RSM or RFM because the satellite orbit is affected by local distortions and the terrain relief [15–18]. As a result, it is important that such systematic errors inherent in the imagery are mitigated by use of polynomial bias-correction models in either image space or object space [19]. The experimental results of the above-mentioned studies showed that the geo-positioning accuracy of QuickBird stereo imageries can be promoted to a sub-pixel accuracy by use of bias-correction models.

However, in above-mentioned studies, the bias was always corrected by refining the RPC-derived ground coordinates, and few studies have focused on bias-correction models for the RSM. In addition, bundle adjustment has been frequently used to simultaneously resolve the interior and exterior parameters of the satellite sensor and ground object coordinates with the aid of GCPs, and this is supposed to achieve the highest geo-positioning accuracy, in theory [20–23]. As a result of the ill-conditioned problem that is caused by strong self-correlation between the position and attitude of the satellite sensor when implementing the bundle adjustment model, the ridge estimation based on Tikhonov regularization technique [24] has often been employed in practice. However, the estimates based on the ridge estimation are intrinsically biased because, in the ridge estimation, the normal equation is substantially changed and the solution algorithm is thus rather complicated and unstable. Therefore, some simpler and more efficient models have been proposed. For example, Teo (2011) presented bias-correction models for the RSM and RFM to evaluate their geo-location performance [7]. In his study, the bias-correction models for the RSM and RFM in the image space were compared by the use of a single scene of QuickBird, WorldView-1, and WorldView-2 imagery. The result showed that the Root Mean Squared (RMS) error for the two-dimensional (2D) geo-location by the use of both the bias-corrected RSM and RFM in the image space was less than 0.1 m. Therefore, in this paper, we further investigate the accuracy of three-dimensional (3D) geo-positioning based on the bias-corrected RSMs and RFMs of QuickBird stereo imagery. In the paper, bias used in our study refers to the error in the exterior orientation, particularly in attitude determination. Therefore, according to the studies presented in [12–15], these biases could be corrected by the use of the polynomial models. This paper is aim to present a comparison of performance of bias-corrected RSMs and RFMs for geo-positioning of QuickBird stereo imageries in both image and object spaces. The compared bias-corrected models include bias-corrected RSM in the orbital space, bias-corrected RSM and RFM in the image space, and bias-corrected RSM and RFM in the object space.

2. Study Area and Data Sources

In the experiments, Shanghai, which is the largest city by population in China, with a large number of very densely populated skyscrapers and high buildings, was chosen as the study area (Figure 1). At the same time, across-track stereo pairs of basic QuickBird panchromatic images, which covered around 324 km^2 of the city of Shanghai, were used. The stereo imageries were collected

on 15 February 2004, and 5 May 2004, with an overlapping area of 95.495%. The vendor-provided parameters of the RPCs and the RSM for each image were supplied in a metadata file with the image. Table 1 shows detail information of QuickBird stereo imageries used in this paper, including the acquisition time, scan direction, view angles, elevation angles, percentage cloud cover, and image spatial resolution. In Figure 1, the two polygons indicate the regions of the QuickBird stereo pairs in the study area.

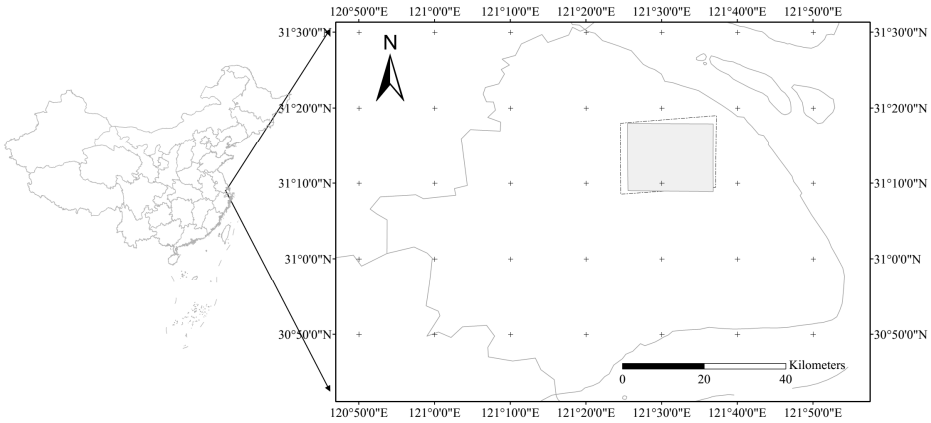

Figure 1. Study area for the experiments.

Table 1. Details of the QuickBird stereo images in the study area.

Image Information	Left Image Of The Stereo Pair	Right Image of the Stereo Pair
Acquisition time	2004-02-15 UTC	2004-05-05 UTC
Scan direction	Forward	Forward
Along-track view angle (°)	19.800	14.600
Cross-track view angle (°)	−5.500	19.600
Off-nadir view angle (°)	20.600	24.400
Elevation angle (°)	64.000	68.200
Percent cloud cover (%)	0.000	0.000
Spatial resolution (m)	0.676	0.708

For the experiments, a total of 84 GCPs were surveyed with a VRS (Virtual Reference Station) RTK-GPS in Shanghai, and the accuracy of these control points was better than 5 cm. Figure 2 shows the QuickBird image and distribution of GCPs and CKPs. In the figure, the black dots and triangulation points represent the GCPs and check points (CKPs), respectively. At the same time, the image coordinates of these control points were carefully measured with accuracy of better than 0.5 pixel.

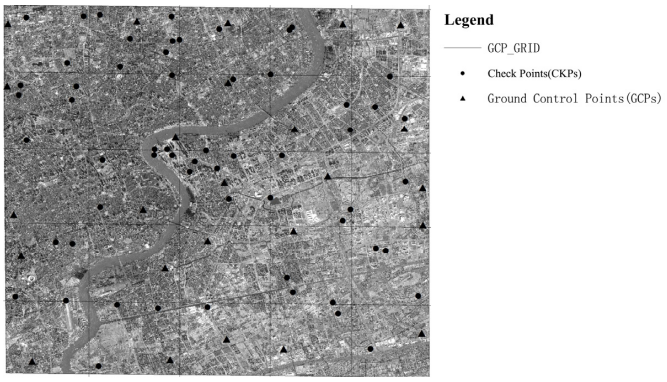

Figure 2. QuickBird image and distribution of the GCPs and CKPs.

3. Framework

Figure 3 shows the entire framework for the comparison of performance of geo-positioning of bias-corrected RSMs and RFMs based on QuickBird stereo imageries. In the proposed framework, there are three main components, as follows, (1) a comparison of geo-positioning accuracy of non-corrected RSM and RFM; (2) a comparison of geo-positioning accuracy of bias-corrected RSMs and RFMs in five scenarios (*i.e.*, bias-corrected RSM in orbital space, bias-corrected RSM and RFM in the image space, and bias-corrected RSM and RFM in object space); and (3) a comparison of performance of different bias-correction models in RSMs and RFMs. The methods are discussed in detail in the following sections.

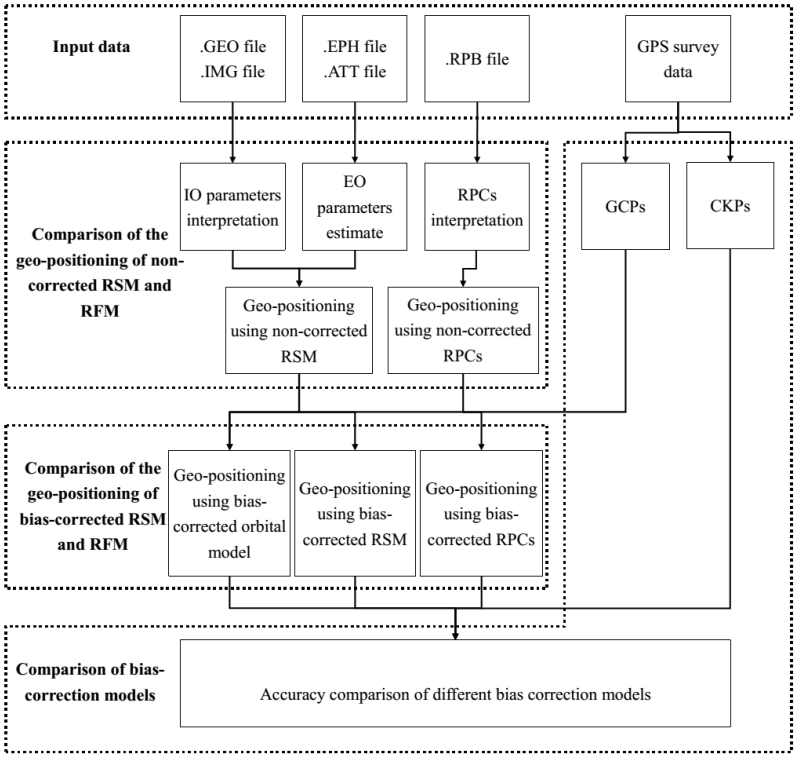

Figure 3. Framework for the comparison of the performance of the bias-corrected RSMs and RFMs.

3.1. Geo-Positioning of the Non-Corrected RSM and RFM

3.1.1. Geo-Positioning of the Non-Corrected RSM

The RSM refers to a model that builds up the transformation between the object and image spaces using onboard data of the HRSI. All the parameters of the RSM can be interpreted from these onboard data. Assuming that the ground coordinates of a point are (X, Y, Z), and that the corresponding image coordinates of this point are (s, l) , then the most commonly used RSM for linear push-broom images can be expressed by:

$$\begin{aligned} s - s_0 &= f\frac{r_{11}(X - X_S) + r_{12}(Y - Y_S) + r_{13}(Z - Z_S)}{r_{31}(X - X_S) + r_{32}(Y - Y_S) + r_{33}(Z - Z_S)} \\ l - l_0 &= f\frac{r_{21}(X - X_S) + r_{22}(Y - Y_S) + r_{23}(Z - Z_S)}{r_{31}(X - X_S) + r_{32}(Y - Y_S) + r_{33}(Z - Z_S)} \end{aligned} \quad (1)$$

where f is the focal length of the camera s_0 and l_0 are the image coordinates of the principal point, and these parameters are defined as the interior orientation (IO) parameters. In addition, X_S, Y_S and Z_S are the coordinates of the satellite position or the center of the sensor frame, r_{ij} (i = 1, 2, 3; j = 1, 2, 3)

are the elements of the rotation matrix with the three angles (j, w, k), and these parameters are defined as the Exterior Orientation (EO) parameters. Furthermore, the EO parameters can be represented by third-order polynomials with time t by:

$$\begin{aligned} X_S &= X_0 + m_1 t + n_1 t^2 + o_1 t^3 \\ Y_S &= Y_0 + m_2 t + n_2 t^2 + o_2 t^3 \\ Z_S &= Z_0 + m_3 t + n_3 t^2 + o_3 t^3 \\ \omega &= \omega_0 + m_4 t + n_4 t^2 + o_4 t^3 \\ \varphi &= \varphi_0 + m_5 t + n_5 t^2 + o_5 t^3 \\ \kappa &= \kappa_0 + m_6 t + n_6 t^2 + o_6 t^3 \end{aligned} \tag{2}$$

where (m_i, n_i, o_i), (i = 1, 2, $\cdots$; 6) are a specific set of coefficients that can be determined by the use of bundle adjustment. A more detailed discussion of the transformation model between the object and image spaces can be found in DigitalGlobe [25]. On the basis of the reconstructed transformation model of the RSM, the coordinates of a point in the object can be derived by use of a forward intersection.

3.1.2. Geo-Positioning of the Non-Corrected RFM

The RFM performs the transformation between the image and object spaces through a ratio of two third-order polynomials. Assuming that the normalized image coordinates of a point are (r, c), and the corresponding normalized ground coordinates are (U, V, W), then the RFM can be expressed by:

$$r = \frac{P_1(U,V,W)}{P_2(U,V,W)}, c = \frac{P_3(U,V,W)}{P_4(U,V,W)} \tag{3}$$

where P_i (U, V, W) (i = 1, 2, 3) is a third-order polynomial and is expressed by:

$$\begin{aligned} P(U,V,W) = \; & e_0 + e_1 U + e_2 V + e_3 W + e_4 U^2 + e_5 UV + e_6 UW + e_7 V^2 + e_8 VW + e_9 W^2 \\ & + e_{10} U^3 + e_{11} U^2 V + e_{12} U^2 W + e_{13} UV^2 + e_{14} UVW + e_{15} UW^2 + e_{16} V^3 \\ & + e_{17} V^2 W + e_{18} VW^2 + e_{19} W^3 \end{aligned} \tag{4}$$

where e_i (i = 1, 2, $\cdots$; 19) are the coefficients of the RPCs provided with the imagery.

3.2. Geo-Positioning of the Bias-Corrected RSM and RFM

As a result of errors in geometric orientation with vendor provided RPCs and RSMs, bias will also exist in the geo-positioning. Furthermore, the discrepancies between measured and nominal coordinates in image space can be express as polynomials of the image coordinates [26–28]. Therefore, four bias-correction models (*i.e.*, shift correction model, shift and scale correction model, affine correction model, and second-order polynomial correction model) in image space or object space are adopted for compensation of the bias in RSMs and RPCs. At the same time, three bias-correction models (*i.e.*, zero-order polynomial model, first-order polynomial model, and second-order polynomial model of the sampling time t relative to the EO parameters of the first scan line in orbital space), with the aim being to compare the impact of different-order polynomial models in orbital space on the geo-positioning accuracy.

Assuming that Ds and Dl are the discrepancies between the nominal and measured coordinates in image space, thus they can be written as follows [15]:

$$\begin{aligned} \Delta s &= a_{10} + a_{11} s + a_{12} l + a_{13} sl + a_{14} s^2 + a_{15} l^2 + \cdots \\ \Delta l &= a_{20} + a_{21} s + a_{22} l + a_{23} sl + a_{24} s^2 + a_{25} l^2 + \cdots \end{aligned} \tag{5}$$

The parameters of the four bias correction models for RSM in image space are described as follows. (1) The shift correction model has two parameters (a_{10}, a_{20}); (2) the shift and scale correction

model has four parameters (a_{10}, a_{11}, a_{20}, a_{21}); (3) the affine correction model has six parameters (a_{10}, a_{11}, a_{12}, a_{20}, a_{21}, a_{22}); and (4) the second-order polynomial correction model twelve parameters ($a_{10}, a_{11}, \cdots; a_{15}, a_{20}, a_{21}, \cdots; a_{25}$).

Assuming that DX, DY, and DZ are the discrepancies between the nominal and measured coordinates in object space, thus they can be express as following [26]:

$$\begin{aligned}\Delta X &= a_{10} + a_{11}X + a_{12}Y + a_{13}Z + a_{14}XY + a_{15}YZ + a_{16}XZ + a_{17}X^2 + a_{18}Y^2 + a_{19}Z^2 + \cdots \\ \Delta Y &= a_{20} + a_{21}X + a_{22}Y + a_{23}Z + a_{24}XY + a_{25}YZ + a_{26}XZ + a_{27}X^2 + a_{28}Y^2 + a_{29}Z^2 + \cdots \\ \Delta Z &= a_{30} + a_{31}X + a_{32}Y + a_{33}Z + a_{34}XY + a_{35}YZ + a_{36}XZ + a_{37}X^2 + a_{38}Y^2 + a_{39}Z^2 + \cdots\end{aligned} \quad (6)$$

The parameters of the four bias correction models for RSM in object space are listed as follows. (1) The shift correction model has three parameters (a_{10}, a_{20}, a_{30}); (2) the shift and scale correction model has six parameters ($a_{10}, a_{11}, a_{20}, a_{21}, a_{30}, a_{31}$); (3) the affine correction model has nine parameters (a_{10}, a_{11}, a_{12}, a_{20}, a_{21}, a_{22}, a_{30}, a_{31}, a_{32}) and (4) the second-order polynomial correction model thirty parameters ($a_{10}, a_{11}, \cdots; a_{19}, a_{20}, a_{21}, \cdots; a_{29}, a_{30}, a_{31}, \cdots; a_{39}$).

Assuming that DX_S, DY_S, DZ_S, Df_S, Dw_S and Dk_S are the discrepancies between the nominal and measured value in orbital space, thus they can be expressed by [26]:

$$\begin{aligned}\Delta X_S &= X_{S_{10}} + X_{S_{11}}t + X_{S_{12}}t^2 + \cdots \\ \Delta Y_S &= Y_{S_{10}} + Y_{S_{11}}t + Y_{S_{12}}t^2 + \cdots \\ \Delta Z_S &= Z_{S_{10}} + Z_{S_{11}}t + Z_{S_{12}}t^2 + \cdots \\ \Delta \phi_S &= \phi_{S_{10}} + \phi_{S_{11}}t + \phi_{S_{12}}t^2 + \cdots \\ \Delta \omega_S &= \omega_{S_{10}} + \omega_{S_{11}}t + \omega_{S_{12}}t^2 + \cdots \\ \Delta \kappa_S &= \kappa_{S_{10}} + \kappa_{S_{11}}t + \kappa_{S_{12}}t^2 + \cdots\end{aligned} \quad (7)$$

The parameters of the three bias correction models for RSM in the orbital space are listed as follows. (1) The zero-order correction model has six parameters ($X_{S_{10}}$, $Y_{S_{10}}$, $Z_{S_{10}}$, $f_{S_{10}}$, $k_{S_{10}}$, $w_{S_{10}}$); (2) the first-order correction model has twelve parameters ($X_{S_{10}}$, $Y_{S_{10}}$, $Z_{S_{10}}$, $f_{S_{10}}$, $k_{S_{10}}$, $w_{S_{10}}$, $X_{S_{11}}$, $Y_{S_{11}}$, $Z_{S_{11}}$, $f_{S_{11}}$, $k_{S_{11}}$, $w_{S_{11}}$); and (3) the second-order correction model has eighteen parameters ($X_{S_{10}}$, $Y_{S_{10}}$, $Z_{S_{10}}$, $f_{S_{10}}$, $k_{S_{10}}$, $w_{S_{10}}$, $X_{S_{11}}$, $Y_{S_{11}}$, $Z_{S_{11}}$, $f_{S_{11}}$, $k_{S_{11}}$, $w_{S_{11}}$, $X_{S_{12}}$, $Y_{S_{12}}$, $Z_{S_{12}}$, $f_{S_{12}}$, $k_{S_{12}}$, $w_{S_{12}}$). Similarly, the parameters of four bias correction models for RFM in image space and object space are the same as those presented in Equations (5) and (6), respectively.

In order to assess the performance of the different bias-correction models, the CKPs are used. The discrepancies between the known and calculated coordinates of the CKPs are first obtained, and this is followed by computation of the RMS error of the CKPs. The $RMS(X)$, $RMS(Y)$ and $RMS(Z)$ are the RMS errors in latitude, longitude, and height, respectively.

4. Results and Analysis

In the experiments, each bias-correction model as introduced in Section 3.2 was performed based on the minimum number of GCPs, and additional GCPs were then added to evaluate the influence of GCPs configuration on the geo-positioning accuracy of bias-corrected RSM and RFM. Furthermore, for each bias-correction model, a free-network adjustment solution with inner constraints was used to evaluate the best indicator of the overall metric potential of the QuickBird stereo imageries by use of all the GCPs as loosely weighted control points with *a priori* standard deviation (σ = 3 m). A more detailed description of the scenarios of the GCP configurations used in the experiments can be found in [28].

4.1. Results of Geo-Positioning Accuracy of Non-Corrected RSM and RFM

In this section, all the points surveyed by GPS were used as CKPs to check the geo-positioning accuracy of the onboard data and the sensor-oriented RPCs. Table 2 shows the result of geo-positioning accuracy of non-corrected RSM and RFM based on QuickBird stereo imageries,

as discussed in Section 3.1. From the results of non-corrected RSM and RFM, it indicated that significant bias exists in the calculated coordinates by the use of non-corrected RSM and RFM. In addition, the geo-positioning accuracies of QuickBird stereo imageries based on non-corrected RSM are 12.398 m in horizontal direction and 21.158 m in vertical direction, and those based on non-corrected RFM are 12.524 m and 21.186 m, respectively. The accuracy difference between non-corrected RFM and RSM is less than 0.2 m in horizontal direction, which is consistent with the report from [7]. However, the biggest difference occurring in vertical direction reaches 1 m.

Table 2. Comparison of the results of geo-positioning accuracy based on non-corrected RSM and RFM.

Model	Number of GCPs/CKPs	Maximum Difference (m)			RMS Error (m)		
		Latitude	Longitude	Height	Latitude	Longitude	Height
RSM	0/84	13.366	27.555	20.936	12.398	21.158	15.295
RFM	0/84	13.604	27.543	21.927	12.524	21.186	16.300

4.2. Results of Geo-Positioning Accuracy of Bias-Corrected RSM and RFM

Five scenarios with different bias-corrected RSM and RFM models were designed to evaluate the accuracy of geo-positioning based on QuickBird stereo imageries. The proposed scenarios were as follows. (1) Scenario one, geo-positioning accuracy of the bias-corrected RSM in orbital space; (2) Scenario two, geo-positioning accuracy of bias-corrected RSM in image space; (3) Scenario three, geo-positioning accuracy of bias-corrected RSM in object space; (4) Scenario four, geo-positioning accuracy of bias-corrected RFM in image space; and (5) Scenario five, geo-positioning accuracy of bias-corrected RFM in object space.

4.2.1. Scenario One, results of Geo-Positioning Accuracy of Bias-Corrected RSM in Orbital Space

Table 3 shows the results of geo-positioning accuracy of bias-corrected RSM by use of three correction models. From the results presented in Table 3, we can see that the geo-positioning accuracy improved with increase in the number of GCPs. An accuracy of 0.8 m in the horizontal direction was achieved in the case of three GCPs in zero-order polynomial correction model in the orbital space. When the number of GCPs was six, the accuracy reached 0.67 m (better than 1 pixel) in planimetry by the use of zero- and first-order polynomial correction models.

Table 3. Results of geo-positioning accuracy of bias-corrected RSM by use of three correction models in orbital space.

Correction Model	Number of GCPs/CKPs	Maximum Difference between the Measured Coordinates and the Calculated Coordinates of the CKPs (m)			RMS Error of the CKPs (m)		
		Latitude	Longitude	Height	Latitude	Longitude	Height
Zero-order polynomial model	3/81	1.932	1.452	3.712	0.645	0.483	1.353
	4/80	1.280	1.351	3.091	0.493	0.444	1.321
	5/79	1.232	1.335	3.279	0.473	0.440	1.358
	6/78	1.046	1.351	3.099	0.438	0.445	1.363
	9/75	1.174	1.119	2.814	0.468	0.343	1.144
	13/71	0.995	0.989	2.831	0.405	0.306	1.104
	25/59	1.077	0.849	2.771	0.405	0.304	0.996
	σ = 3 m	0.933	0.873	2.998	0.425	0.294	0.948
First-order polynomial model	6/78	1.199	1.074	2.894	0.479	0.375	1.284
	9/75	1.184	0.945	2.729	0.528	0.325	1.024
	13/71	1.155	0.884	2.719	0.455	0.315	0.986
	25/59	1.090	0.802	2.432	0.432	0.321	0.840
	σ = 3 m	0.932	0.805	2.104	0.428	0.295	0.806

Table 3. *Cont.*

Correction Model	Number of GCPs/CKPs	Maximum Difference between the Measured Coordinates and the Calculated Coordinates of the CKPs (m)			RMS Error of the CKPs (m)		
		Latitude	Longitude	Height	Latitude	Longitude	Height
Second-order Polynomial model	9/75	1.213	0.949	2.564	0.533	0.323	0.984
	13/71	1.164	0.885	2.738	0.490	0.330	0.983
	25/59	0.987	0.793	2.078	0.445	0.322	0.788
	σ = 3 m	1.039	0.816	2.181	0.422	0.294	0.729

4.2.2. Scenario Two, Results of Geo-Positioning Accuracy of Bias-Corrected RSM in Image Space

Table 4 shows the results of geo-positioning accuracy by use of these four models performed in image space. From the results presented in Table 4, we can see that, with shift and scale bias-correction model and three GCPs, the geo-positioning accuracy of QuickBird stereo pairs significantly improved to 0.520 m in latitude, 0.564 m in longitude, and 1.160 m in height, which was close to the accuracy achieved by the use of all 84 GCPs.

Table 4. Results of geo-positioning accuracy of bias-corrected RSM by use of four correction models in image space.

Correction Model	Number of GCPs/CKPs	Maximum Difference between the Measured Coordinates and Calculated Coordinates of the CKPs (m)			RMS Error of the CKPs (m)		
		Latitude	Longitude	Height	Latitude	Longitude	Height
Shift model	1/83	1.504	3.611	8.220	0.640	1.946	3.393
	3/81	1.342	4.298	9.407	0.680	2.160	4.130
	4/80	1.349	3.436	6.575	0.690	1.894	2.876
	5/79	1.303	3.470	6.356	0.673	1.909	2.951
	6/78	1.328	3.585	6.591	0.665	1.937	2.910
	9/75	1.355	3.580	6.653	0.660	1.907	2.885
	13/71	1.446	3.578	6.447	0.623	1.931	3.000
	25/59	1.416	3.324	6.047	0.618	1.851	2.849
	σ = 3 m	1.542	3.927	7.165	0.615	1.939	2.993
Shift and scale model	3/81	1.392	1.513	3.171	0.520	0.564	1.160
	4/80	1.310	1.453	2.933	0.561	0.524	1.181
	5/79	1.261	1.416	3.166	0.543	0.520	1.188
	6/78	1.247	1.343	2.855	0.536	0.508	1.184
	9/75	1.206	1.268	2.416	0.529	0.490	0.995
	13/71	1.293	1.264	2.533	0.496	0.501	0.950
	25/59	1.251	1.017	2.540	0.482	0.502	0.859
	σ = 3 m	1.352	1.308	2.425	0.509	0.511	0.904
Affine model	3/81	1.605	1.159	3.051	0.589	0.435	1.142
	4/80	1.252	1.158	2.741	0.500	0.416	1.225
	5/79	1.200	1.109	2.961	0.479	0.407	1.229
	6/78	1.255	1.134	2.826	0.503	0.392	1.251
	9/75	1.174	0.985	2.593	0.476	0.337	1.055
	13/71	0.999	0.910	2.588	0.413	0.318	0.984
	25/59	0.934	0.821	2.428	0.398	0.319	0.828
	σ = 3 m	0.938	0.844	2.506	0.432	0.308	0.855
Second-order polynomial model	6/78	1.970	1.991	3.555	0.854	0.716	1.617
	9/75	0.995	1.183	2.712	0.457	0.363	1.007
	13/71	0.851	1.035	2.646	0.403	0.333	0.966
	25/59	0.934	0.821	2.428	0.406	0.319	0.845
	σ = 3 m	0.894	0.839	1.923	0.367	0.301	0.811

4.2.3. Scenario Three, Results of Geo-Positioning Accuracy of Bias-Corrected RFM in Image Space

Table 5 shows the results of geo-positioning accuracy by use of four correction methods performed in image space. From Table 5, we can see that the four RFM correction models in image space achieved an accuracy that was close to bias-correction models of RSM in image space.

Table 5. Results of geo-positioning accuracy of bias-corrected RFM by use of four correction methods in image space.

Correction Model	Number of GCPs/CKPs	Maximum Difference between the Measured Coordinates and the Calculated Coordinates of the CKPs (m)			RMS Error of CKPs (m)		
		Latitude	Longitude	Height	Latitude	Longitude	Height
Shift model	1/83	1.696	4.032	7.175	0.607	2.231	3.151
	3/81	1.359	4.810	9.588	0.668	2.452	4.434
	4/80	1.345	3.853	6.350	0.673	2.125	2.981
	5/79	1.223	3.881	6.366	0.612	2.144	2.993
	6/78	1.137	3.969	6.835	0.548	2.174	2.877
	9/75	1.147	3.989	6.767	0.593	2.143	2.878
	13/71	1.120	3.975	6.661	0.557	2.171	2.965
	25/59	1.089	3.842	6.231	0.560	2.082	2.910
	σ = 3 m	1.440	4.063	7.321	0.554	2.173	2.991
Shift and scale model	3/81	1.306	1.479	3.855	0.484	0.556	1.487
	4/80	1.268	1.411	3.413	0.560	0.516	1.302
	5/79	1.150	1.364	3.411	0.499	0.513	1.309
	6/78	0.990	1.312	2.805	0.448	0.506	1.279
	9/75	1.076	1.215	2.738	0.483	0.485	1.070
	13/71	0.973	1.229	2.768	0.452	0.495	1.060
	25/59	0.947	1.016	2.750	0.439	0.507	0.924
	σ = 3 m	1.054	1.204	2.600	0.464	0.509	0.984
Affine model	3/81	1.532	1.156	4.067	0.543	0.476	1.459
	4/80	1.147	1.207	3.663	0.524	0.446	1.363
	5/79	1.026	1.265	3.650	0.459	0.442	1.369
	6/78	0.962	1.320	2.988	0.409	0.436	1.353
	9/75	1.019	1.173	2.829	0.448	0.369	1.114
	13/71	0.945	1.092	2.815	0.405	0.349	1.092
	25/59	0.866	0.964	2.787	0.389	0.345	0.945
	σ = 3 m	0.990	0.922	2.976	0.416	0.337	0.960
Second-order polynomial model	6/78	3.461	4.113	4.068	1.642	1.969	1.371
	9/75	0.983	1.381	2.518	0.403	0.400	0.973
	13/71	1.055	1.213	2.455	0.370	0.362	0.918
	25/59	1.029	0.976	2.157	0.376	0.347	0.749
	σ = 3 m	0.967	0.919	2.221	0.346	0.328	0.777

4.2.4. Scenario Four, Results of Geo-Positioning Accuracy of Bias-Corrected RSM in Object Space

Table 6 shows the results of geo-positioning accuracy for bias-corrected RSM by four methods performed in object space. From Table 6, we can see that some larger errors occurred in affine correction model when the number of GCPs was four or five. Furthermore, the computation did not converge in second-order polynomial model when the number of GCPs was 13. Overall, the results showed that second-order and higher-order polynomial models might not be suitable for performing geo-positioning of RSM in object space.

Table 6. Results of geo-positioning accuracy of bias-corrected RSM by use of four correction methods in object space.

Correction Model	Number of GCPs/CKPs	Maximum Difference between the Measured Coordinates and the Calculated Coordinates of the CKPs (m)			RMS Error of CKPs (m)		
		Latitude	Longitude	Height	Latitude	Longitude	Height
Shift model	1/83	1.497	4.072	7.745	0.619	2.138	3.386
	3/81	1.355	4.784	8.866	0.666	2.329	4.022
	4/80	1.334	3.889	6.724	0.665	2.047	2.787
	5/79	1.294	3.914	6.504	0.653	2.063	2.859
	6/78	1.288	4.047	6.692	0.652	2.095	2.828
	9/75	1.261	4.014	6.797	0.644	2.056	2.787
	13/71	1.342	3.998	6.597	0.614	2.080	2.897
	25/59	1.318	3.592	5.629	0.615	1.993	2.823
	σ = 3 m	1.573	3.995	7.303	0.612	1.914	2.918
Shift and scale model	3/81	1.514	1.779	3.509	0.544	0.701	1.280
	4/80	1.287	1.692	3.257	0.571	0.646	1.311
	5/79	1.250	1.657	3.494	0.560	0.645	1.318
	6/78	1.274	1.578	3.170	0.555	0.635	1.329
	9/75	1.295	1.519	2.778	0.552	0.620	1.142
	13/71	1.361	1.521	2.893	0.522	0.635	1.098
	25/59	1.326	1.298	2.910	0.520	0.646	1.057
	σ = 3 m	1.424	1.351	2.617	0.529	0.594	1.034
Affine model	4/80	6.274	1.294	6.725	1.354	0.455	1.671
	5/79	5.875	1.254	8.772	1.281	0.462	2.027
	6/78	1.733	1.498	5.004	0.574	0.464	1.472
	9/75	2.146	1.548	6.783	0.619	0.427	1.678
	13/71	3.560	1.932	6.140	0.839	0.514	1.565
	25/59	0.951	1.191	3.208	0.406	0.412	1.011
	σ = 3 m	0.937	0.860	2.560	0.406	0.313	0.865
Second-order polynomial model	13/71	inv	inv	inv	inv	inv	inv
	25/59	5.711	8.824	30.073	1.172	1.304	5.376
	σ = 3 m	0.845	0.872	1.934	0.306	0.338	0.798

4.2.5. Scenario Five, the Results of Geo-Positioning Accuracy of Bias-Corrected RFM in Object Space

Table 7 shows the results of geo-positioning accuracy of bias-corrected RFM by four correction models performed in object space. From the results presented in Table 7, we can see that the four correction models performed are similar as scenario four.

Table 7. Results of geo-positioning accuracy of bias-corrected RFM by use of four correction methods in object space.

Correction Model	Number of GCPs/CKPs	Maximum Difference between the Measured Coordinates and the Calculated Coordinates of the CKPs (m)			RMS Error of the CKPs (m)		
		Latitude	Longitude	Height	Latitude	Longitude	Height
Shift model	1/83	1.800	4.075	6.777	0.634	2.110	3.085
	3/81	1.527	4.782	9.109	0.712	2.313	4.346
	4/80	1.470	3.893	6.480	0.687	2.015	2.909
	5/79	1.357	3.918	6.495	0.636	2.031	2.922
	6/78	1.170	3.989	6.967	0.583	2.054	2.810
	9/75	1.300	4.001	6.889	0.623	2.022	2.805
	13/71	1.201	3.972	6.787	0.594	2.044	2.887
	25/59	1.226	3.585	5.973	0.594	1.949	2.820
	σ = 3 m	1.592	4.088	7.438	0.594	1.882	2.937

Table 7. *Cont.*

Correction Model	Number of GCPs/CKPs	Maximum Difference between the Measured Coordinates and the Calculated Coordinates of the CKPs (m)			RMS Error of the CKPs (m)		
		Latitude	Longitude	Height	Latitude	Longitude	Height
Shift and scale model	3/81	1.359	1.672	4.224	0.505	0.683	1.576
	4/80	1.339	1.582	3.782	0.565	0.629	1.392
	5/79	1.230	1.547	3.786	0.516	0.630	1.402
	6/78	1.113	1.520	3.198	0.475	0.629	1.370
	9/75	1.158	1.430	3.131	0.506	0.613	1.183
	13/71	1.072	1.453	3.165	0.478	0.632	1.170
	25/59	1.033	1.278	3.150	0.472	0.646	1.066
	σ = 3 m	1.093	1.328	2.915	0.485	0.594	1.091
Affine model	4/80	4.850	1.224	6.527	1.066	0.434	1.768
	5/79	5.331	1.325	5.342	1.167	0.481	1.609
	6/78	6.003	1.362	6.477	1.305	0.478	1.720
	9/75	1.982	1.590	3.226	0.571	0.415	1.218
	13/71	3.196	2.012	3.023	0.762	0.517	1.192
	25/59	1.026	1.205	3.987	0.399	0.396	1.132
	σ = 3 m	0.866	0.902	2.965	0.379	0.301	0.959
Second-order polynomial model	13/71	inv	inv	inv	inv	inv	inv
	25/59	5.875	8.422	32.980	0.990	1.314	5.349
	σ = 3 m	0.948	0.895	2.210	0.309	0.295	0.755

4.3. Comparison and Discussion of the Performance of Bias-Correction Models of the RSM and RFM

In this section, based on the experimental results of above-mentioned five scenarios, a comprehensive comparison is conducted with regard to the performance of bias-correction models of the RSM and RFM in image space, object space, and orbital space.

4.3.1. Comparison of the Performance of Bias-Correction Models

In Scenario one, three bias-correction models as introduced in Section 3.2 were tested to examine the impact of different-order polynomials on geo-positioning accuracy of QuickBird stereo imageries in orbital space. At the same time, in Scenarios two to five, four bias-correction models as introduced in Section 3.2 were tested to see if they could improve the geo-positioning accuracy of both RSM and RFM in image and object spaces. In order to compare the performance of these seven bias-correction models, the results of geo-positioning accuracy of tested QuickBird stereo imageries were calculated by use of all 84 GCPs. The comparison of the performance of these seven bias-correction models is discussed as follows.

(1) From the results in Table 3, we can see that all three bias-correction models presented a good performance in geo-positioning accuracy, and second-order polynomial model achieved highest accuracy of 0.5 m in horizontal direction and 0.7 m in vertical direction.

(2) From Tables 4–7 it can be seen that shift bias-correction model is an efficient model. In Scenarios two to five, the results of geo-positioning accuracy by use of shift bias-correction model with only one GCP show that the geo-positioning accuracy has been greatly improved and reached 2.3 m in horizontal direction and 3.4 m in vertical direction. At the same time, the highest accuracy of 0.7 m in latitude was achieved. However, the accuracy was not greatly improved with an increase in the number of GCPs.

(3) From Tables 4–7 it can be seen that shift and scale correction model is one of the most stable models in the geo-positioning performance of RSM and RFM in both image and object spaces. By use of three well-distributed GCPs, the geo-positioning achieved sub-pixel accuracy in planimetry. In addition, the geo-positioning accuracy reached 0.5 m in horizontal direction and about 1.0 m in vertical direction as the number of GCPs increased to 25.

(4) From Tables 4–7 affine bias-correction model achieved the highest accuracy of 0.398 m in latitude, 0.319 m in longitude, and 0.828 m in height with respect to bias-corrected RSM in the image space when the GCPs reached 25 points. However, a poorer performance was observed in the experiments with bias-corrected RSM and RFM in the object space when the number of GCPs was less (for example, three GCPs in Table 6 and four GCPs in Table 7).

(5) From Tables 4–7 it can be seen that second-order polynomial correction model obtained the highest accuracy of 0.376 m in latitude, 0.347 m in longitude, and 0.749 m in height with respect to bias-corrected RFM in image space when the GCPs reached 25 points. However, the computation did not converge in the experiments with the bias-corrected RSM and RFM in object space when the number of GCPs was 13, as shown in Tables 6 and 7.

4.3.2. Comparison of the Performance of Bias-Correction Spaces

In this section, the performance of bias-correction models in different spaces—the orbital space, the image space, and the object space based on 25 GCPs—is discussed. Figure 4 shows a comparison of the results of geo-positioning accuracy by use of bias-correction models of both RSM and RFM in three spaces, based on 25 GCPs.

We can see from the Figure 4 that, (1) the results of geo-positioning accuracy by use of three polynomial correction models, as described in Section 3.2, in orbital space are stable and consistent in three directions. In addition, the results are also close to those of four bias-correction models as introduced in Section 3.2 of RSM and RFM in image space; (2) Better accuracies of geo-positioning by use of bias-correction models in image space were achieved than those in object space, and the second-order polynomial bias-correction model accomplished the worst accuracy in height.

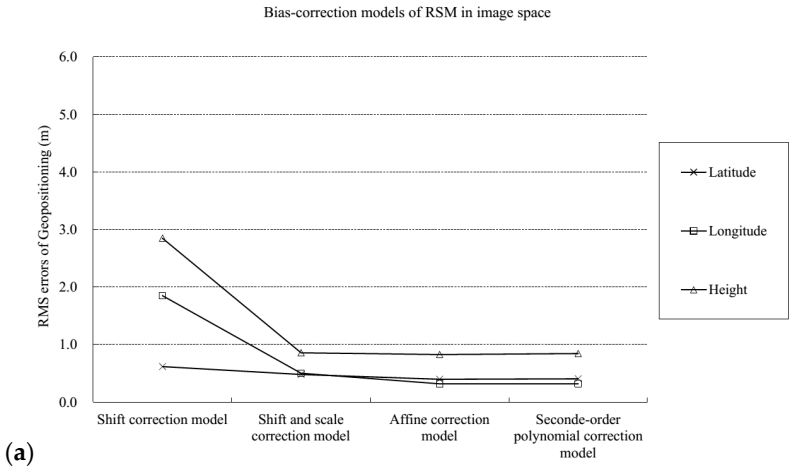

(**a**)

Figure 4. *Cont.*

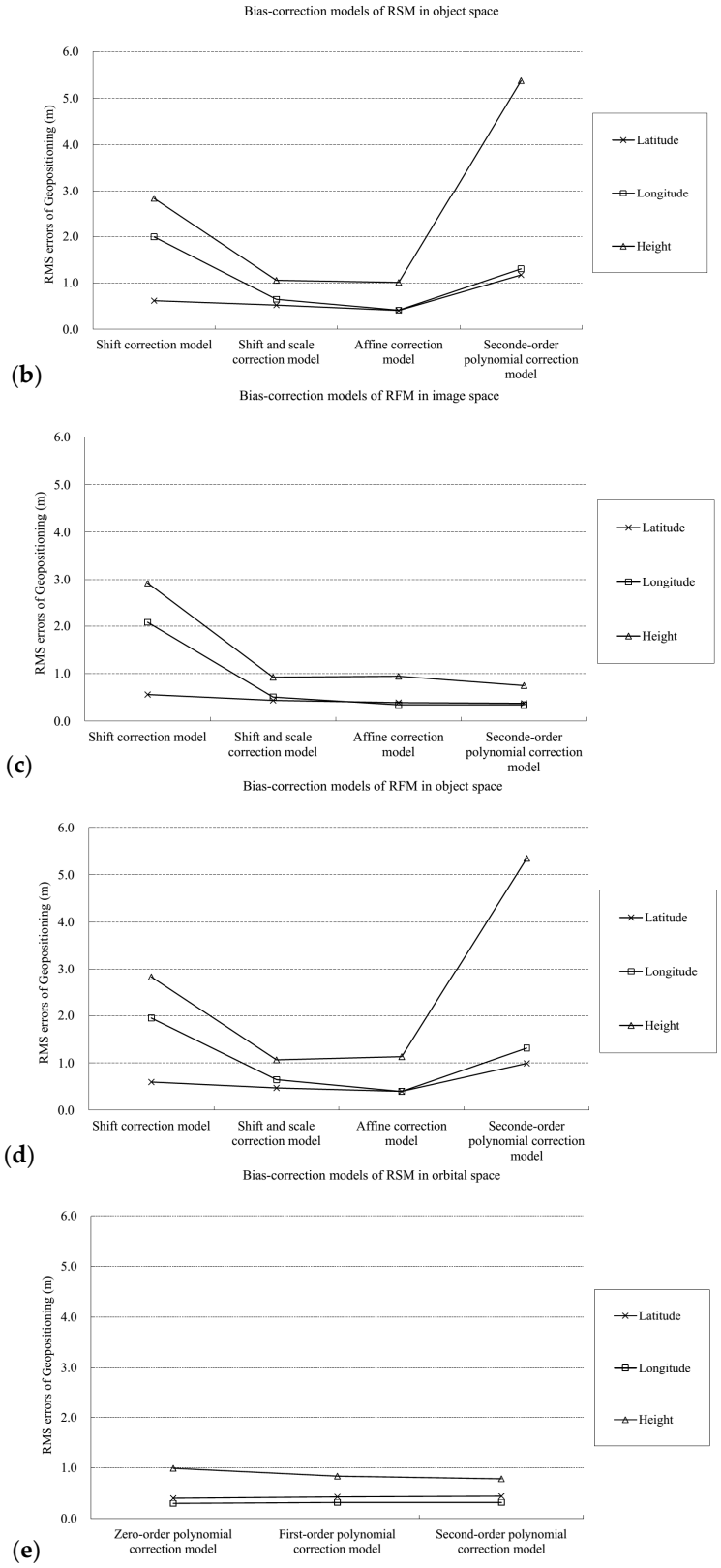

Figure 4. Comparison of the results of the geo-positioning accuracy by use of bias-correction models of both RSM and RFM in three spaces, based on 25 GCPs. (**a**) The results of bias-correction models of RSM in image space; (**b**) The results of bias-correction models of RSM in object space; (**c**) The results of bias-correction models of RFM in image space; (**d**) The results of bias-correction models of RFM in object space; (**e**) The results of bias-correction models of RFM in orbital space.

4.3.3. Comparison of the Performance of Bias-Correction of Geometric Sensor Models

In this section, we compare the geo-positioning accuracy with respect to different bias-correction models with different geometric sensor models (*i.e.*, RSM and RFM) in both image and object spaces. Figure 5 shows a comparison of the performance of geo-positioning accuracy with respect to the different bias-correction models and geometric sensor models (*i.e.*, RSM and RFM) in both image and object spaces. The RMS error of the coordinates of CKPs is calculated by $\sqrt{\left((\mathrm{D}latitude)^2+(\mathrm{D}longitude)^2+(\mathrm{D}height)^2\right)/n}$, where n is the number of CKPs, D*longitude*, D*latitude*, and D*height* represent the discrepancies of calculated and measured coordinates of CKPs in latitude, longitude, and height, respectively. From the Tables 2–7 we can see that by use of affine bias-correction model or shift and scale bias-correction model, the performance of geo-positioning accuracy with RSM was better than that of RFM in both image space and object space, except for the cases of shift bias-correction model and second-order polynomial bias-correction model with respect to the RSM and RFM. In addition, the accuracy difference between the two geometric sensor models was less than 0.1 m.

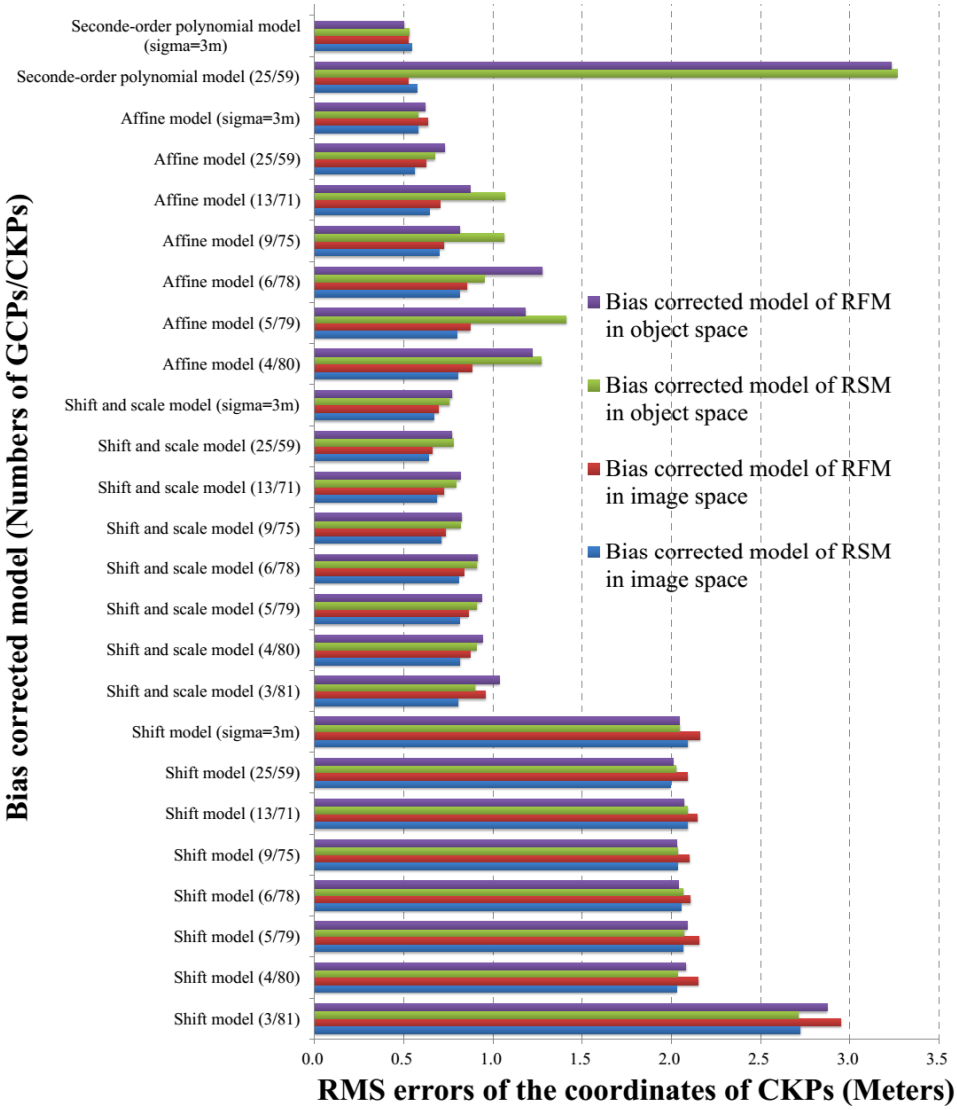

Figure 5. Comparison of the performance of geo-positioning accuracy with respect to different bias-correction models and geometric sensor models.

5. Conclusions

This paper has presented a comparison of performance of bias-corrected RSM and RFM models for geo-positioning of QuickBird stereo images. These compared models referred to bias-corrected RSM in orbital space, bias-corrected RSM and RFM in image space, and bias-corrected RSM and RFM in object space. The experimental results indicated that:

(1) By use of zero-order polynomial correction model in orbital space and a minimum of three GCPs, the refined RPCs improved the accuracy to 0.8 m in planimetry and 1.3 m in height, which indicates that the low-order correction model in orbital space can accurately reduce the effects of ephemeris and attitude errors.

(2) The geo-positioning accuracy with RSM was better than that of RFM in both image and object spaces by use of bias correction models, and the low-order correction models (such as affine model, shift and scale model) can achieve a sub-pixel accuracy in horizontal direction with a few number of GCPs (for example, one to three GCPs).

(3) High-order polynomial correction models (such as second-order polynomial model) performed rather unstable, particularly in object space.

Acknowledgments: This paper was substantially supported by the National Natural Science Foundation of China (Project No. 41325005, 41401489 and No. 41401531), National High-tech Research and Development Program (Project No. 2012AA121302), China Special Funds for Meteorological and Surveying, Mapping and Geoinformation Research in the Public Interest (Project No. GYHY201306055 and No. HY14122136), Shanghai Foundation for University Youth Scholars (Project No. ZZHY13033), and Innovation Program of Shanghai Municipal Education Commission (Project No. 15ZZ082).

Author Contributions: The concept and design of framework for bias-corrected RSMs and RFMs for the geo-positioning of high-resolution satellite stereo imagery were proposed by Zhonghua Hong. The investigation on the methods for bias-corrected RSMs and RFMs was performed by Xiaohua Tong, and Shijie Liu. The experiments were performed by Peng Chen, Huan Xie and Yanmin Jin. All authors have contributed significantly and have participated sufficiently to take the responsibility for this research. Moreover, all authors are in agreement with the submitted and accepted versions of the publication.

Conflicts of Interest: The authors declare no conflict of interest.

References

1. Kim, T.; Dowman, I.J. Comparison of two physical sensor models for satellite images. *Photogramm. Rec.* **2006**, *21*, 110–123. [CrossRef]
2. Poli, D. A rigorous model for spaceborne linear array sensors. *Photogramm. Eng. Remote Sens.* **2007**, *73*, 187–196. [CrossRef]
3. Tao, C.V.; Hu, Y. 3D reconstruction methods based on the rational function model. *Photogramm. Eng. Remote Sens.* **2002**, *68*, 705–714.
4. Di, K.C.; Ma, R.J.; Li, R.X. Geometric processing of Ikonos stereo imagery for coastal mapping applications. *Photogramm. Eng. Remote Sens.* **2003**, *69*, 873–879.
5. Kim, T.; Kim, H.; Rhee, S. Investigation of physical sensor models for modeling SPOT 3 orbits. *Photogramm. Rec.* **2007**, *22*, 257–273. [CrossRef]
6. Weser, T.; Rottensteiner, F.; Willneff, J.; Poon, J.; Fraser, C.S. Development and testing of a generic sensor model for pushbroom satellite imagery. *Photogramm. Rec.* **2008**, *23*, 255–274. [CrossRef]
7. Teo, T.A. Bias Compensation in a Rigorous Sensor Model and Rational Function Model for High-Resolution Satellite Images. *Photogramm. Eng. Remote Sens.* **2011**, *77*, 1211–1220. [CrossRef]
8. Li, R.; Zhou, F.; Niu, X.; Di, K. Integration of Ikonos and QuickBird imagery for geopositioning accuracy analysis. *Photogramm. Eng. Remote Sens.* **2007**, *73*, 1067–1074.
9. Habib, A.; Kim, K.; Shin, S.W.; Kim, C.; Bang, K.I.; Kim, E.M.; Lee, D.C. Comprehensive analysis of sensor modeling alternatives for high-resolution imaging satellites. *Photogramm. Eng. Remote Sens.* **2003**, *73*, 1241–1251. [CrossRef]
10. Li, R.; Niu, X.T.; Liu, C.; Wu, B.; Deshpande, S. Impact of imaging geometry on 3D geopositioning accuracy of stereo IKONOS imagery. *Photogramm. Eng. Remote Sens.* **2009**, *75*, 1119–1125. [CrossRef]

11. Robertson, B. Rigorous geometric modeling and correction of QuickBird imagery. In Proceedings of the 2003 IEEE International Geoscience and Remote Sensing Symposium, Toulouse, France, 21–25 July 2003; pp. 21–25.
12. Fraser, C.S.; Hanley, H.B. Bias compensated RPCs for sensor orientation of high-resolution satellite imagery. *Photogramm. Eng. Remote Sens.* **2005**, *71*, 909–915. [CrossRef]
13. Tong, X.H.; Liu, S.J.; Weng, Q.H. Geometric processing of QuickBird stereo imageries for urban land use mapping, a case study in Shanghai, China. *IEEE J. Sel. Top. Appl. Earth Obs. Remote Sens.* **2009**, *2*, 61–66. [CrossRef]
14. Tong, X.H.; Liu, S.J.; Weng, Q.H. Bias-corrected rational polynomial coefficients for high accuracy geo-positioning of QuickBird stereo imagery. *ISPRS J. Photogramm. Remote Sens.* **2010**, *65*, 218–226. [CrossRef]
15. Grodecki, J.; Dial, G. Block adjustment of high-resolution satellite images described by rational polynomials. *Photogramm. Eng. Remote Sens.* **2003**, *69*, 59–68. [CrossRef]
16. Liu, S.; Fraser, C.S.; Zhang, C.; Ravanbakhsh, M.; Tong, X. Georeferencing performance of THEOS satellite imagery. *Photogramm. Rec.* **2011**, *26*, 250–262. [CrossRef]
17. Poli, D.; Toutin, T. Review of developments in geometric modelling for high resolution satellite pushbroom sensors. *Photogramm. Rec.* **2012**, *27*, 58–73. [CrossRef]
18. Zhang, Y.; Wang, B.; Zhang, Z.; Duan, Y.; Zhang, Y.; Sun, M.; Ji, S. Fully automatic generation of geoinformation products with Chinese ZY-3 satellite imagery. *Photogramm. Rec.* **2014**, *29*, 383–401. [CrossRef]
19. Fraser, C.S.; Hanley, H.B. Bias compensation in rational functions for IKONOS satellite imagery. *Photogramm. Eng. Remote Sens.* **2003**, *69*, 53–58. [CrossRef]
20. Noguchi, M.; Fraser, C.S.; Nakamura, T.; Shimono, T.; Oki, S. Accuracy assessment of QuickBird stereo imagery. *Photogramm. Rec.* **2004**, *19*, 128–137. [CrossRef]
21. Orun, A.B.; Natarajan, K. A bundle adjustment software for SPOT imagery and photography, Tradeoff. *Photogramm. Eng. Remote Sens.* **1994**, *60*, 1431–1437.
22. Li, R. Potential of high-resolution satellite imagery for National Mapping Products. *Photogramm. Eng. Remote Sens.* **1998**, *64*, 1165–1169.
23. Toutin, T. Comparison of stereo-extracted DTM from different high-resolution sensors, SPOT-5, EROS-A, IKONOS-II and QuickBird. *IEEE Trans. Geosci. Remote Sens.* **2004**, *42*, 2121–2129. [CrossRef]
24. Tikhonov, A.N.; Arsenin, V.Y. *Solutions of Il l-Posed Problems*; Wiley: New York, NY, USA, 1977.
25. DitigalGlobe. *QuickBird Imagery Products—Product Guide, Revision 4.7.3*; DitigalGlobe, Inc.: Longmont, CO, USA, 2007.
26. Wang, J.; Di, K.; Li, R. Evaluation and improvement of geopositioning accuracy of IKONOS stereo imagery. *J. Surv. Eng.* **2005**, *13*, 35–42. [CrossRef]
27. Fraser, C.S.; Dial, G.; Grodecki, J. Sensor orientation via RPCs. *ISPRS J. Photogramm. Remote Sens.* **2006**, *60*, 182–194. [CrossRef]
28. Tong, X.H.; Hong, Z.H.; Liu, S.J.; Zhang, X.; Xie, H.; Li, Z.Y.; Yang, S.L.; Wang, W.A.; Bao, F. Building-damage detection using pre- and post-seismic high-resolution IKONOS satellite stereo imagery, a case study of the May 2008 Wenchuan Earthquake. *ISPRS J. Photogramm. Remote Sens.* **2012**, *68*, 13–27. [CrossRef]